Eindhoven University of Technology

MASTER

Neutron shielding design for neutron based parcel scanning system

Winkeler, Rob J.M.

Award date:
2021

Link to publication

Disclaimer
This document contains a student thesis (bachelor's or master's), as authored by a student at Eindhoven University of Technology. Student theses are made available in the TU/e repository upon obtaining the required degree. The grade received is not published on the document as presented in the repository. The required complexity or quality of research of student theses may vary by program, and the required minimum study period may vary in duration.

General rights
Copyright and moral rights for the publications made accessible in the public portal are retained by the authors and/or other copyright owners and it is a condition of accessing publications that users recognise and abide by the legal requirements associated with these rights.

- Users may download and print one copy of any publication from the public portal for the purpose of private study or research.
- You may not further distribute the material or use it for any profit-making activity or commercial gain

Eindhoven University of Technology
Science and Technology of Nuclear Fusion
&
Dynaxion

Neutron shielding design for a neutron based parcel scanning system

Master Thesis

R.J.M. Winkeler

Supervisors:
Maximilian Messmer, Cor Datema, Roger Jaspers

Eindhoven,Tuesday 4th May, 2021

Redaction information

This thesis was carried out in collaboration with the company Dynaxion and parts of the thesis have been classified as confidential. Information which was determined as critical for Dynaxion has been redacted from this publicly available report. These parts have been marked as `<redacted>` in the thesis. The graduation committee responsible for the grading of the student had access to the full report to make a qualitative assessment of the student. For more information please contact the academic supervisor.

Abstract

Current safety screening methods for suitcases and parcels mainly rely on x-ray imaging. With this technique the contents can only be judged based on the density and shape of materials. Dynaxion is a startup that develops a neutron based scanning system that measures the relative distribution of certain elements in a parcel to accurately detect prohibited substances. Neutrons are produced with a DD neutron generator and shot at a parcel where gammas are produced due to inelastic scattering and capture reactions. Radiation from the neutron beam and subsequent emitted gammas needs to be shielded. The shielding needs to be designed for the neutron source and system geometry, and because Dynaxion sells a commercial product the solution should be optimized for size, cost, and portability.

The aim of this work is to find and computationally test potential neutron shielding materials and design a neutron shield with those materials. From literature, potential shielding materials were selected. A numerical neutron transport model was implemented in Matlab to obtain a ranked list of shielding materials based on neutron shielding performance. High density polyethylene (HDPE) and borated HDPE were selected as main shielding materials with the possible addition of a `<redacted>` for shielding the highest energy neutrons. With this knowledge, a shielding geometry around the existing system setup was designed, consisting of a collimator, beam dump, and system enclosure. This design was implemented and tested using the Monte Carlo code MCNP. It was found that by optimizing the beam collimator and beam dump, a `<redacted>` cm thick layered hull consisting of borated and non borated HDPE is sufficient to reduce the neutron flux from the source by the required 10 orders of magnitude.

Contents

Contents **iv**

1 Introduction **1**
1.1 Context . . . 1
1.2 Problem statement . . . 1

2 Theoretical background **3**
2.1 Slowing down neutrons . . . 3
2.2 Absorbing neutrons . . . 4
2.3 Neutron transport . . . 4
2.3.1 Transport cross section . . . 4
2.3.2 Diffusion theory . . . 5
2.4 Commonly used shielding materials . . . 6
2.5 Neutron source . . . 6

3 Neutron shielding materials **9**
3.1 Neutron transport model . . . 9
3.1.1 Two species model . . . 9
3.1.2 Molecules as shielding material . . . 11
3.1.3 Exceptional case of hydrogenous materials . . . 11
3.2 Verification . . . 12
3.3 Materials . . . 14

4 Simulation configuration **17**
4.1 MCNP . . . 17
4.2 Design process . . . 17
4.3 Source Implementation . . . 18
4.4 Source Bias . . . 18
4.5 Geometry . . . 19
4.6 Materials . . . 20
4.7 Tally . . . 20
4.8 Simulation . . . 21

5 Neutron shielding design **22**
5.1 Design requirements . . . 22
5.2 Collimator . . . 23
5.2.1 Simple collimator . . . 23
5.2.2 Beam shaping . . . 26
5.2.3 Volume optimization . . . 28
5.3 Parcel . . . 29
5.3.1 Results . . . 31
5.4 Beam stop . . . 32

5.4.1 Results 33
5.4.2 Volume optimization 34
5.5 Overall shielding 35

6 Conclusion **38**

Bibliography **40**

Chapter 1

Introduction

1.1 Context

Searching for security threads in parcels and suitcases is done with non-invasive x-ray screening. This technique can identify objects within the package based on their density and shape. But the resulting images cannot always give a conclusive answer as to what is inside. When a parcel is suspected to contain drugs or explosives, it has to be checked manually or with a detection dog. All these steps take time, are costly and have a high false alarm rate.

Dynaxion is a start-up that is tackling this problem by developing a commercial scanning system based on neutron inelastic scattering. A scheme for this system roughly looks as follows: Firstly, a particle accelerator accelerates deuterium ions to an energy of 3.85 MeV. These ions subsequently hit a deuterium target where a proportion of the accelerated deuterons fuse with target deuterons. One product of this fusion reaction is a high energy neutron of 2.45 MeV. Because of the incident particles kinetic energy, the resulting neutrons have an energy distribution ranging from 1.6 MeV to 7.1 Mev with an increasing probability for increasing energy. Additionally, this kinetic energy also ensures that the direction of the neutrons leaving the source is not uniformly distributed over 4π. Instead, the angular distribution of neutrons is skewed in the forward direction. This way, a neutron source is created with the intensity and neutron energy peaking in the forward direction.

Next, a package is positioned in the forward direction of the neutron radiation. Depending on the cross sections, some neutrons interact with the atoms of the package. Those neutrons either scatter or are absorbed. The reactions of interest are inelastic scattering and neutron capture, because it leaves the atoms in an excited state after which they decay by emitting gamma radiation. The energy of these gamma rays is element dependent and thus their detection reveals the presence of distinct atoms in the package. Finally, a neural network classifies the contents based on the measured radiation spectra which materials are present at what position.

1.2 Problem statement

The use of many high energy neutrons is necessary to induce enough gamma rays to determine the contents of a parcel quickly. But the neutron radiation and the resulting gamma radiation pose a safety hazard for humans and machines. Therefore, this dangerous radiation needs to be kept within the system. On the other hand, packages have to enter and exit the system. This raises conflicting goals, especially because radiation can leave through the smallest cracks while packages have sizes in the order of decimeters.

Solutions to this problem are not only limited by design constraints that ensure proper operation of the principles stated above. Also market research has resulted in a few requirements that the system should meet to offer future clients a good addition to their current security setup: first, staff should be able to work next to the system without risking dangerous radiation exposure.

Secondly, the throughput of the system should be on the order of 100 to 1000 packages per hour. This value depends on whether the system can be used to check all packages, or only to check the fraction of packages that are deemed suspicious by, for instance, an x-ray system. Thirdly, the system is preferably light, compact, and portable, because package processors are used to changing their conveyor belts and security setup frequently. The target size of the total system is comparable to the size of a shipping container. Finally, the system must be financially viable. It is expected that this means that the system should not cost more than a few million euros. These requirements bring us to the following research question:

Can we design a compact and lightweight radiation shielding for a neutron based scanning system?

Chapter 2

Theoretical background

Neutron radiation degrades materials and is hazardous for humans. Sources of neutron radiation are found at fission and fusion reactors and at particle accelerators. To protect their environments the neutron radiation has to be shielded. Radiation is effectively shielded when the neutron is absorbed in the shielding material. To do that, first the neutron has to be slowed down. How that is done is explained in section 2.1. After slowing down, neutrons are absorbed through a capture reaction, explained in 2.2. For individual neutrons these processes are probabilistic, but in section 2.3 it is explained how the flow of many neutrons through a medium is deterministic. Subsequently, in section 2.4, common neutron shielding materials are introduced and their strong and weak points are analysed in order to find suitable materials for the design. Neutron shielding designs have to be adapted to each particular application, mainly depending on the energy of the incoming neutrons. Section 2.5 explains the Dynaxion neutron source, which determines the energy of neutrons that have to be shielded in this work.

2.1 Slowing down neutrons

Neutrons lose energy when they scatter. This can be either elastic scatter (energy lost by the neutron is transferred to the target particle) or inelastic scatter (the neutron is absorbed and re-emitted and the nucleus is left in an excited state, this generally only happens above 1 MeV). On a hydrogen atom neutrons lose on average half their energy per collision [1]. On heavier elements neutrons lose less energy per collision. To slow fast neutrons to thermal velocity neutrons need to scatter many times. The probability of one scattering reaction taking place is given by the scatter cross section. This value is different for all elements and isotopes and is dependent on the incident neutron energy. A material that is good at slowing down neutrons, that is a good moderator, has a low mass, a high scatter cross section at relevant energies and a high density. Upon collision a neutron transfers a fraction of its momentum and energy to the nucleus. How much energy is transferred depends on the mass of the nucleus and the scattering angle. Considering many collisions of many neutrons, the energy loss per collision can be averaged over all scattering angles. For a certain element the average logarithmic energy decrease is given by [2]:

$$\xi = 1 + \frac{(A-1)^2}{2A} \ln\left(\frac{A-1}{A+1}\right) \tag{2.1}$$

where A is the mass number of the element. The remaining neutron energy after n collisions is now given by: $E = E_0 e^{-\xi n}$. For instance, to slow a typical neutron from 2 MeV to 1 eV it needs 15 collisions with hydrogen, or 92 with carbon, or 1812 with uranium: $n = \frac{\ln(E_0/E_{th})}{\xi}$.

The energy dependent scattering cross section for all isotopes can be found in the ENDF/B database [3]. These cross-sections are given in barn (10^{-24} cm^2) for energies ranging from 10^{-5} eV to 20 MeV and they represent the scattering probability of a neutron with one isotope. To describe the large-scale properties of the medium, the so-called microscopic cross section is multiplied by the

atomic number density of that medium resulting in the macroscopic cross section (often expressed in cm^{-1}):

$$\Sigma_s = N\sigma_s = \frac{\rho N_A}{M}\sigma_s \tag{2.2}$$

where ρ is the specific mass, N_A is the Avogadro constant, M the atomic mass and σ the microscopic cross section. Following a neutron, its energy when moving through a medium is now given by: $E = E_0 e^{-\xi\Sigma_s x}$, where x is the neutrons traveled distance. Note that x is not the distance from the source, due to scattering this can be much smaller. It should be noted though that the microscopic cross section depends on neutron energy so the neutrons energy does not decay strictly exponential.

When the neutrons reach a kinetic energy corresponding to the thermal agitation of the host medium, they either lose or gain energy upon collision. As a result a group of neutrons in this energy range have various speeds following a Maxwellian distribution depending on the temperature of the medium. At 290 K, the most probable neutron energy is 0.025 eV. A neutron that reaches this energy is said to be thermalized. Combining the number of collisions needed to thermalize a neutron with the number of collisions per unit length gives the macroscopic slowing down cross section [4]:

$$\Sigma_1 = \frac{\xi\Sigma_s}{\ln(E_0/E_{th})} \tag{2.3}$$

It represents the probability of neutron thermalizing while traveling through a medium. Starting with a group of monoenergetic neutrons, the number of neutrons that have not yet thermalized as a function of the neutrons traveled distance (note that x is not displacement) is given by [4]:

$$G(x) = G_0 \cdot e^{-\Sigma_1 x} \tag{2.4}$$

2.2 Absorbing neutrons

Neutrons are absorbed through neutron capture reactions: the neutron disappears upon collision and one or more particles, depending on the reaction, are emitted. Many isotopes can absorb a neutron (though for some elements the cross-section relatively small) after which they emit a photon. Hydrogen for instance, emits a 2.223 MeV photon. Some isotopes can on top of that also have a nuclear reaction after which they emit a proton, alpha particle, or other nucleus. One example is ^{10}B that splits in $^{2}_{4}$He and $^{3}_{7}$Li plus a 0.48 MeV photon. Analogous to neutron moderators, a good neutrons absorber has a big absorption cross-section, high atom density, and has easy-to-deal-with reaction products. The probability of a neutron absorption by one nucleus is given by the capture cross section. This capture cross section is also energy dependent and the values for all isotopes can be extracted from the ENDF/B database [3]. The macroscopic cross section is calculated by multiplying the microscopic cross section with the atomic number density: $\Sigma_a = N\sigma_a$. Starting with a group of monoenergetic neutrons, the number of neutrons that have not yet been absorbed as a function of the neutrons traveled distance is given by [4]:

$$G(x) = G_0 \cdot e^{-\Sigma_a x} \tag{2.5}$$

2.3 Neutron transport

2.3.1 Transport cross section

Equation 2.4 and 2.5 describe the energy and flux as a function of traveled distance, neglecting the trajectory change after every collision. However, with scatter reactions, the neutron is only removed from the forward flow when the deflection angle is greater than 90°. The average deflection

angle per collision μ does not depend on neutron energy (with the exception of certain molecules). It is defined as [4]:

$$\mu = \overline{\cos\theta} \approx \frac{2}{3A} \tag{2.6}$$

where θ is the scattering angle, and A is the mass number of the target nucleus. The probability of a neutron being deflected 90 degrees going through a medium is now given by $\Sigma_s(1-\mu)[cm^{-1}]$. Combining the two loss channels gives the macroscopic transport cross section [4]:

$$\Sigma_{tr} = \Sigma_a + \Sigma_s(1-\mu) \tag{2.7}$$

The transport cross section represents the probability of a neutron being removed from the forward flow and can thus be used to calculate neutron beam attenuation:

$$J(x) = J_0 e^{-\Sigma_{tr}x} \tag{2.8}$$

2.3.2 Diffusion theory

Current is the net stream of neutrons through a surface, whereas flux describes the gross number of neutrons passing through a surface. To know what goes in and out of the shielding we need the current. But reaction rates are calculated with neutron flux. To simplify this model, the shielding medium is assumed to be homogeneous and extending to infinity in y and z direction. Consequently there is no net transfer of neutrons in those directions, so the flux is only calculated in the x-direction. Current and flux are related to each other by Fick's first law [5]:

$$J = -D\frac{d\phi}{dx} \tag{2.9}$$

where D is the diffusion coefficient and x the shielding thickness. Note that from here onward, x is not the traveled distance anymore, but shielding thickness. This law is applicable to neutrons with an isotropic directional distribution. The neutron beam that has to be shielded does not have an isotropic directional distribution. But once in the shielding medium, neutrons are quickly 'removed' from the beam due to scatter collisions; it takes far more collisions to slow down (15 with hydrogen) than to change the direction by 90 degrees (3 with hydrogen). Further into the shielding medium the directional distribution is more isotropic. Neutrons leaving the shielding medium likely encounter a material that provides not nearly as much transport resistance as the shielding material. Consequently neutrons do not scatter back and diffusion theory is not valid anymore. To keep this model simple, it is assumed that Fick's law holds in the entire shielding, while keeping in mind that results are an approximation. The approximation will become more unreliable when the shielding thickness is decreased approaching the transport mean free path. As for other applications of diffusion theory, the diffusion coefficient represents the conductance of moving particles through a medium. We have already calculated neutron transport resistance in the form of the transport cross-section. The neutron diffusion coefficient is defined as the inverse of three times the transport cross-section [5]:

$$D = \frac{1}{3\Sigma_{tr}} \tag{2.10}$$

where the factor three comes from the three coordinate components.

The second law that is used to construct the neutron diffusion theory is the conservation of neutrons: change in neutron flow = absorption – production. Combining the neutron conservation law with Fick's law of diffusion gives the neutron diffusion equation [6] [5]:

$$D\frac{d^2\phi}{dx} - \Sigma\phi(x) + S(x) = 0 \tag{2.11}$$

in which Σ is the relevant macroscopic cross section for that loss channel, and S is a source term. It should be noted that neutron-neutron interactions and neutron decay are not included in this theory because effects of these interactions are insignificant to the transport problem.

With this expression the problem of following the neutrons traveled distance instead of the shielding thickness is solved. This is an important results, because neutrons bounce around so their traveled distance is not representative of the net distance between shield entrance and its absorption point.

2.4 Commonly used shielding materials

From this theory on neutron transport, the best performing neutron shielding materials are derived. In literature, for many materials the shielding performance is calculated. These materials often fall in one of the following categories:

- **Concrete** is the most commonly used neutron shielding material [7]. It is so effective because of its high density, effectiveness in gamma shielding, and ability to adjust the composition. By adding certain elements to the mixture, the shielding performance can be adjusted to its application. For instance, by adding boron for better neutron absorption, or adding iron for better stopping power at high neutron energies. The disadvantage of concrete is that it is heavy, and therefore often constructed like a bunker. For this work, however, having to build a bunker does not satisfy the portability requirement.

- **Water** is an effective neutron shielding material because of its high hydrogen content. Compared to concrete it has a low density, potentially resulting in a lighter weight shielding. However, it is not effective in shielding gamma radiation because of its low density. This can be solved by making the water shield thicker and by adding boric acid to produce lower energy gammas in the neutron capture reaction. However, with boric acid the water is difficult to store due to corrosion. [8]

- **Hydrocarbons** like plastics have an hydrogen content which is almost as high as that of water, which makes them excellent in neutron shielding. They are lightweight, leading to a low weight but poor gamma shielding performance, and easily processable. Similar to concrete, the addition of boron increases the shielding performance and causes lower energy gamma radiation.

- **Advanced materials** are designed specially for neutron shielding. They have an as high as possible hydrogen content combined with the optimal amount of boron. This enables shielding to be smaller and lighter [9]. However, these materials often are expensive and not widely used.

For most of these materials, shielding performances are theoretically calculated, and experimentally tested. However, the calculations are always focused on a particular neutron source because the results depend highly on the neutron energy of that source. However, Dynaxion is using a novel neutron source technology, with an incomparable neutron energy spectrum. Therefore, in this work, the neutron shielding performance of different materials is tested for the spectrum of the Dynaxion neutron source. The characteristics of this neutron source are explained in the next section.

2.5 Neutron source

The neutron source of Dynaxion consists of a deuteron accelerator which is aimed at a deuterated titanium target. Deuterons are accelerated by a radio frequency quadrupole particle accelerator to a few MeV, creating a deuteron beam with a 6 mm diameter. The target has a cylindrical shape with the axis oriented in line with the accelerator. It has a thickness of only 0.02

mm and a diameter much larger than the beam diameter. Around the deuterated titanium are a couple of other materials (nickel, steel, water, and aluminium) that assist in the workings of the neutron source, but in this work are only noteworthy because the newly created neutrons have to pass through them.

The energy of an accelerated deuteron is high enough to overcome the coulomb barrier when it hits a stationary deuteron in the target, and thus the two particles fuse. With a fifty percent chance each, either a tritium particle and a proton, or a helium particle and a neutron are formed. The latter fusion reaction is as follows:

$$ {}^{2}_{1}\mathrm{H} + {}^{2}_{1}\mathrm{H} \rightarrow {}^{3}_{2}\mathrm{He}\ (0.82\ \mathrm{MeV}) + {}^{1}_{0}\mathrm{n}\ (2.45\ \mathrm{MeV}) \tag{2.12} $$

To analyse all possible energies and directions of the resulting neutron, the momentum and energy balances are solved. For this, the accelerated deuteron is defined to be particle 1, the stationary deuteron particle 2, the neutron particle 3, and the helium atom particle 4. The initial energy of the accelerated deuteron is E_1, a fusion energy of $E_f = 3.27$ MeV is released, and the masses are approximated to be $m1 = m2 \approx 2$, $m3 \approx 1$ and $m4 \approx 3$. Before the collision, the accelerated deuteron has velocity:

$$ V_1 = \sqrt{\frac{2E_1}{m_1}} \tag{2.13} $$

Because the velocity of the stationary particle is zero, the velocity of the center of mass is:

$$ V_{COM} = \frac{m_1 V_1 + m_2 V_2}{m_1 + m_2} = \frac{V_1}{2} \tag{2.14} $$

We now consider the center of mass frame in which the deuterons have velocity $v_1 = -v_2 = V_1/2$, see figure 2.1. In this frame of reference, the momentum and energy balances are given by:

$$ m_1 v_1 + m_2 v_2 = m_3 v_3 + m_4 v_4 \tag{2.15} $$

and

$$ \frac{1}{2} m_1 v_1^2 + \frac{1}{2} m_2 v_2^2 + E_f = \frac{1}{2} m_3 v_3^2 + \frac{1}{2} m_4 v_4^2 \tag{2.16} $$

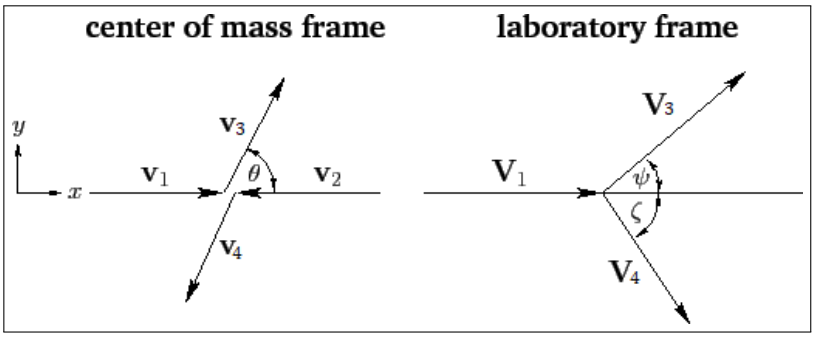

Figure 2.1: Schematic drawing of particle collision in center of mass frame and laboratory frame. Adapted from [10]

Filling in the mass approximations and solving for v_3 and v_4 gives:

$$ v_3 \approx \sqrt{\frac{3}{4} E_1 + \frac{3}{2} E_f} \tag{2.17} $$

and

$$ v_4 \approx -\frac{\sqrt{\frac{3}{4} E_1 + \frac{3}{2} E_f}}{3} \tag{2.18} $$

We are only interested in the neutrons velocity v_3. Depending on whether the collision was head-on or under an angle, the neutrons velocity is directed under any angle θ. Translating this velocity back to the laboratory frame thus yields:

$$V_{3,x} = \sqrt{\frac{3}{4}E_1 + \frac{3}{2}E_f} \cdot \cos\theta + \sqrt{\frac{1}{4}E_1} \tag{2.19}$$

and

$$V_{3,y} = \sqrt{\frac{3}{4}E_1 + \frac{3}{2}E_f} \cdot \sin\theta \tag{2.20}$$

All possible outcomes are mapped by filling in $0° \leq \theta \leq 180°$ and $0 \leq E_1 \leq 3.85$ MeV, and plotted in figure 2.2.

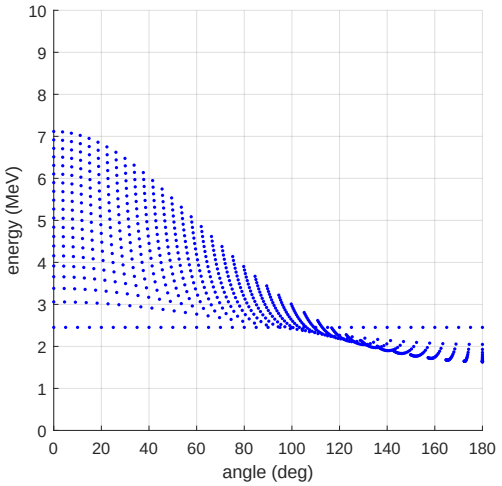

Figure 2.2: Possible outcomes of equations 2.19 and 2.20 for $0 \leq \theta \leq 180$ and $0 \leq E_1 \leq 3.85$ MeV.

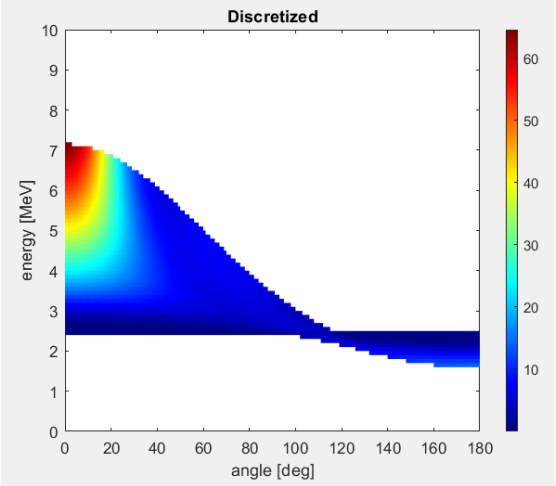

Figure 2.3: Dynaxion source spectrum. The angle represents the deviation from the axis of the axisymmetric source, with 0 degrees being the forward direction. This spectrum is the result of many fusion reactions between accelerated deuterons (in the forward direction) and stationary target deuterons.

The fusion cross section is higher when the kinetic energy of the deuteron is higher. Therefore, the points in figure 2.2 that belong to E_1 close to 3.85 MeV are more probable. Similarly, a glancing collision, resulting in the neutron going close to an angular direction of 0°, is more probable than a head-on collision. The probabilities are not calculated analytically. However, Dynaxion has provided the results of this calculation that were done with the DROSG code. The resulting energy spectrum is depicted in figure 2.3. This is the neutron spectrum that has to be shielded, and is used in the rest of this work. It is important to note that these directions only represent neutrons leaving the source. After this, collisions force neutrons to follow a different angle and only a few collisions are needed to entirely change direction. It is therefore not possible to design shielding in each direction individually with a 1 dimensional calculation. In the next chapter a neutron transport model is made to overcome this problem.

Chapter 3

Neutron shielding materials

In order to test the performance of different shielding materials for the relevant neutron energies, a model is created in Matlab to solve the diffusion equation. The model is explained in section 3.1 and verified in section 3.2. From a literature study a list of potential neutron shielding materials is assembled in section 3.3. These materials are run through the model to test which material has the best shielding performance.

3.1 Neutron transport model

Solving the diffusion equation (equation 2.11) involves calculating the macroscopic cross section of the shielding material of interest. This comes with the following challenges:

- The cross sections are energy dependent, meaning that the stopping power of a material changes while the neutron is being stopped.
- Most materials have a much lower absorption cross section than scatter cross section. As a result, neutrons bounce around a lot before they get absorbed. Therefore, neutron diffusion must be added to the equation.
- For compound materials and molecules, every isotope influences the shielding characteristics. How big their contribution to the moderation or absorption is, is also energy dependent.

These effects can be taken into account by solving the neutron diffusion equation for two groups of neutrons: fast neutrons ($E > 0.025$ eV) and thermal neutrons ($E \approx 0.025$ eV). For the fast neuron group, the macroscopic cross sections are averaged over the energy range. When fast neutrons have thermalized, they are removed from the fast neutron group and added to the thermal neutron group.

3.1.1 Two species model

In a group of neutrons the slowing down and absorption processes happen simultaneously. Every individual neutron follows its own path. With a Monte-Carlo simulation method all these paths are calculated separately, but this simplified model works with average behavior. In most materials, scatter reactions are predominant over capture reactions. Therefore, for most neutrons it holds that they scatter many times and are thermalized before they are absorbed. At this point slowing down and absorption processes do not happen simultaneously anymore because on average, thermalized neutrons do not lose energy.

To still be able to model both processes the group of neutrons can be divided into two groups. One group of fast neutrons, with a higher than thermal energy, that are slowed down and have a low chance of being absorbed. And a second group with thermal neutrons that bounce around without losing energy. This group loses its neutrons only due to absorption and is repleted by thermalized neutrons from the fast group.

Fast neutron group

Fast neutrons originate directly from a neutron source. As an approximation the model assumes monoenergetic, monodirectional neutrons with an energy of 7 MeV. The current in the forward direction impinging on the target is $J_0 = 10^5$ n/cm^2/s. Within the shield there is no fast neutron source. Fast neutrons are lost through two different loss channels.

The loss channel with the highest cross section is thermalization. Its probability is given by the macroscopic slowing down cross section (Σ_1), see section 2.1. The second loss channel is neutron capture, which is called resonance absorption in this energy range. Its probability is given by the macroscopic absorption cross section (Σ_a). With the source and loss channels of the fast group determined, the neutron diffusion equation is [5]:

$$\frac{d^2\phi_f}{dx^2} - \frac{\Sigma_1}{D_f}\phi_f(x) - \frac{\Sigma_{af}}{D_f}\phi_f(x) = 0 \tag{3.1}$$

Both cross sections and the diffusion coefficient are energy dependent. The variables $\frac{\Sigma_1}{D}$ and $\frac{\Sigma_a}{D}$ are averaged over the energy range, from 0.025 eV to 7 Mev. Since neutrons need as many collisions to go from 1 MeV to 1 keV as from 1 keV to 1eV, the average is weighted accordingly.

For neutron moderators in fission reactors it can often be assumed that resonance absorption is negligible, causing the third term to disappear. In this case the slowing down power of the medium is given by one constant, called the Fermi age (τ) or moderation length (L_f): $\tau = L_f^2 = \frac{D_f}{\Sigma_1}$

Boundary conditions

The diffusion equation can be solved with the addition of two boundary conditions. Firstly, the current of the neutrons J_0 entering the shield at $x = 0$ is fixed: $\frac{d\phi_f(0)}{dx} = -\frac{D}{J_0}$. For the second boundary condition, it is assumed that the medium outside of the shield has a much lower density than the shielding material itself. Neutrons that leave the shield do not scatter back. Consequently, the flux near the surface of the shield is very an-isotropic, which means that diffusion theory does not hold in the surface region. The true flux at the border can be approximated by setting the flux at an extrapolation length from the shield to zero. From neutron transport theory an extrapolation length of $2.13D$ was obtained. Therefore the second boundary condition is $\phi_f(t + 2.13D_f) = 0$, where t is the thickness of the shield.

For some shielding materials, for instance boron, the resonance absorption cannot be neglected. But with graphite, for instance, the solution does not differ much from the case where resonance absorption is neglected. In that case the neutron flux as function of shield thickness is given by [5]:

$$\phi_f(x) = \frac{J_0 L_f}{D} e^{-x/L_f} \tag{3.2}$$

The fast neutron current out of the shield can now be calculated again using Fick's law [5]:

$$J_f(x) = -D\frac{d\phi_f}{dx} = J_0 e^{-x/L_f} \tag{3.3}$$

This expression does not differ much from the neutron thermalization function from the first subsection. Effectively, the exponent has changed from Σ_1 to $\sqrt{\Sigma_1/D_f}$. What this change effectively does is compensating for the fact that neutrons bounce around and thus the net distance they travel is shorter than the total traveled distance.

Thermal neutron group

The thermal neutrons in the shield originate from fast neutrons that are thermalized. Where they are thermalized exactly is described by the first loss term of the fast neutron flux. Thermal neutrons are lost only through absorption reactions, the probability of which is given by the macroscopic absorption cross section. The thermal neutron diffusion equation is thus given by [5]:

$$\frac{d^2\phi_{th}}{dx^2} - \frac{\Sigma_{ath}}{D_{th}}\phi_{th}(x) + \frac{\Sigma_1}{D_f}\phi_f(x) = 0 \tag{3.4}$$

Again two boundary conditions are needed to solve the equation. Since the influx of neutrons was assumed to be mono-energetic, no thermal neutrons enter the shield. Therefore, on both sides of the shield, the flux at an extrapolation distance from the surface is set to zero: $\phi_{th}(-2.13D_{th}) = 0$ and $\phi(t + 2.13D_{th}) = 0$. And analogous to the fast neutron group, a characteristic decay length, called diffusion length, is given by: $L_d^2 = \frac{\Sigma_{ath}}{D_{th}}$.

Also the thermal neutron diffusion equation is solved in Matlab with symbolic functions. The exact solution from the negligible resonance absorption case is also available:

$$\phi_{th}(x) = \phi_{th}(0) \cdot e^{-x/L_d} + \frac{\Sigma_1\phi_f(0)}{D_{th}(L_f^2 - L_d^2)} \cdot \left(e^{-x/L_d} - e^{-x/L_f}\right) \tag{3.5}$$

3.1.2 Molecules as shielding material

For shielding material that only includes one element the interaction cross sections are imported from the ENDF/B database and used in all the formulas above. For compound materials or molecules the cross sections have to be combined as follows: firstly, the macroscopic cross section is calculated for every compound in the molecule. An example with water is presented below:

$$\Sigma^H = \frac{2 \cdot \rho^{H_2O} N_A}{M^{H_2O}}\sigma^H \quad and \quad \Sigma^O = \frac{1 \cdot \rho^{H_2O} N_A}{M^{H_2O}}\sigma^O \tag{3.6}$$

Note that the density and molar mass of the total molecule is used. The numeric values in the nominator represent the number of atoms of that compound in the molecule. Subsequently, the macroscopic cross sections of the compounds are added to obtain the macroscopic cross section of the molecule. This addition rule applies to all cross sections: scatter, absorption and transport.

$$\Sigma^{H_2O} = \Sigma^H + \Sigma^O \tag{3.7}$$

To calculate the average logarithmic energy decrement of the molecule the weighted average of all individual compounds is taken as follows:

$$\xi^{H_2O} = \frac{\xi^H\Sigma^H + \xi^O\Sigma^O}{\Sigma^H + \Sigma^O} \tag{3.8}$$

3.1.3 Exceptional case of hydrogenous materials

When the kinetic energy of the neutrons is in the same order or lower than the chemical binding energy of a molecule the total scatter cross section is not the sum of all individual cross sections. In this case the neutron does not 'see' the individual atoms but rather the total molecule. For hydrogenous materials the chemical binding energy is high enough that the effect takes place already around the thermal energy of the neutrons, this has a big effect on the diffusion of thermal neutrons. To still properly model neutron behavior around thermal energies, the ENDF/B database [11] also provides data of microscopic scatter cross section (σ_s) and the average value of the cosine of the angle in the lab system (μ) for some hydrogenous materials: H_2O and polyethylene, among others. Figure 3.1 shows the influence of the chemical binding energy of water on the two variables as a function of neutron energy.

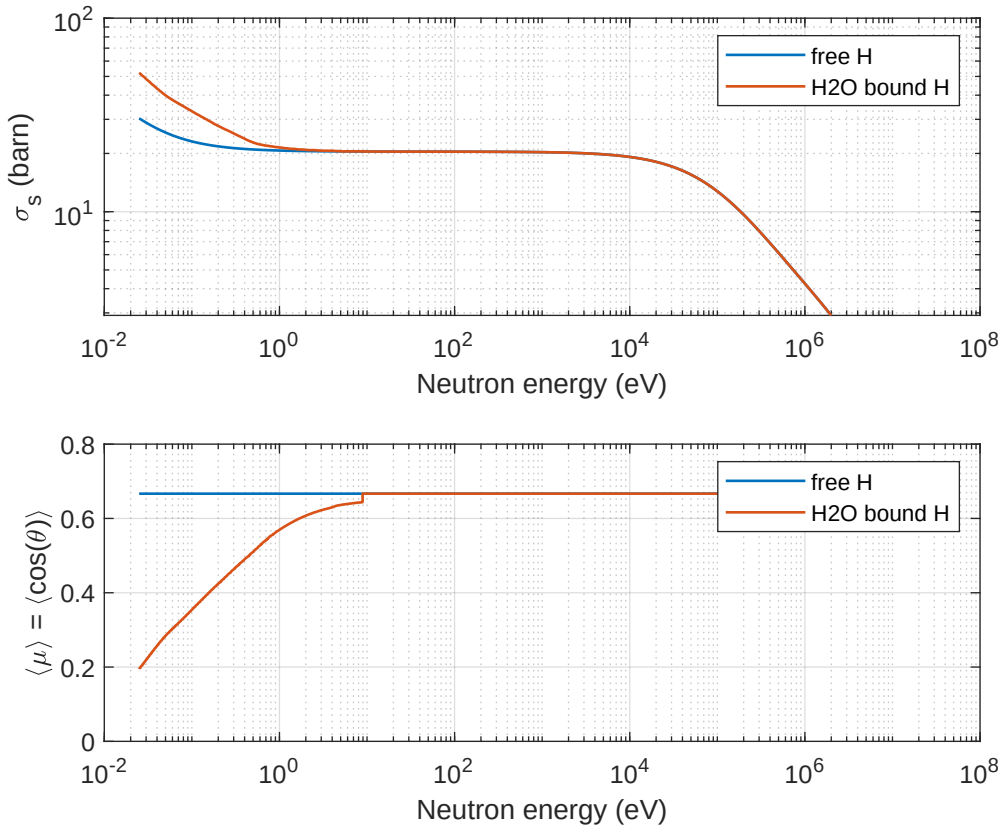

Figure 3.1: Influence of chemical binding energy of water on σ_s and $\langle\mu\rangle$ as function of incident neutron energy (eV) compared to free hydrogen.

3.2 Verification

The model that has been made consist of two parts. The first part averages the variables that are used for the differential equation over all the relevant energies. And the second part solves the neutron diffusion equations. To verify the first part, the calculated averages are compared to numbers that can be found in literature [12], see table 3.1. Initially this is done for graphite, because it is a single element material and it is widely studied as moderator for fission reactors. The averages are calculated for neutrons slowing down from 2 MeV (average fission neutron energy) to 0.025 eV.

To verify the second part, the model outcome is compared to the exact solution of the negligible resonance absorption case. Graphite has a very small absorption cross section, especially at high energies, so the neglected absorption is expected to have a very small influence on the outcome. Other differences between the model and the exact solution are the boundary conditions at the back side of the shield. The exact solution sets the neutron flux to zero at infinity, whereas this model uses the extrapolation distance. It should be noted that exact solution in this case means the algebraic solution the differential equation with certain boundary conditions and assumptions, and thus it is not necessarily a more accurate representation of reality. For the first comparison the boundary conditions of the model have been matched with the exact solution.

	Σ_s	Σ_a	Σ_{tr}	D	L
Fast					
Literatur	0.360	-	0.340	1.016	17.30
Model	0.362	$3.48 \cdot 10^{-5}$	0.342	1.006	18.73
deviation	-1%		-1%	1%	-8%
Thermal					
Literature	0.385	0.00036	0.36	0.917	50.00
Model	0.398	0.00031	0.38	0.887	53.32
deviation	-3%	14%	-6%	3%	-7%

Table 3.1: Comparison of model variables between the Matlab model and values found in literature for slowing down a 2 MeV neutron to 0.025 eV in graphite.

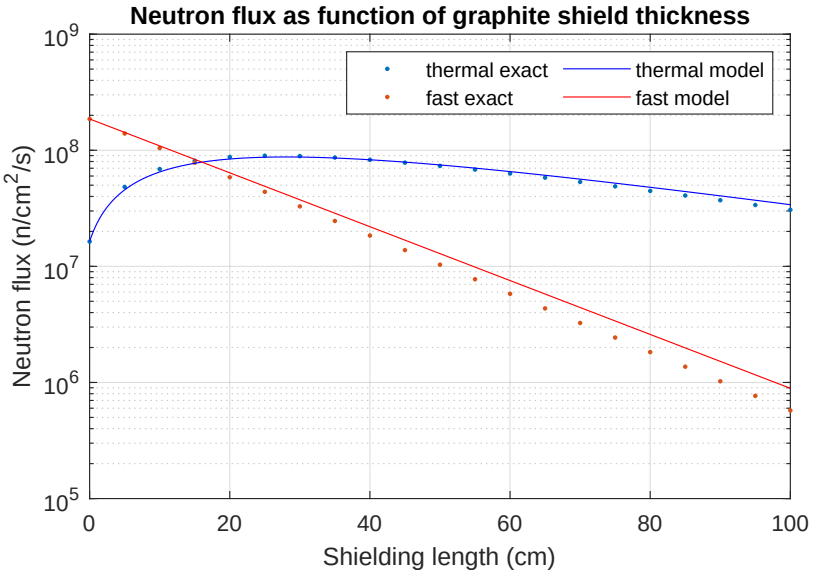

Figure 3.2: Neutron flux as function of graphite shield thickness of the fast and thermal neutron group, comparing transport model results with exact theoretical values.

A second comparison is done with proper boundary conditions in the model, but with the exact solution unchanged. What we are really interested in is the neutron current leaving the shield at the back. It is calculated with Fick's law, and the results are as follows:

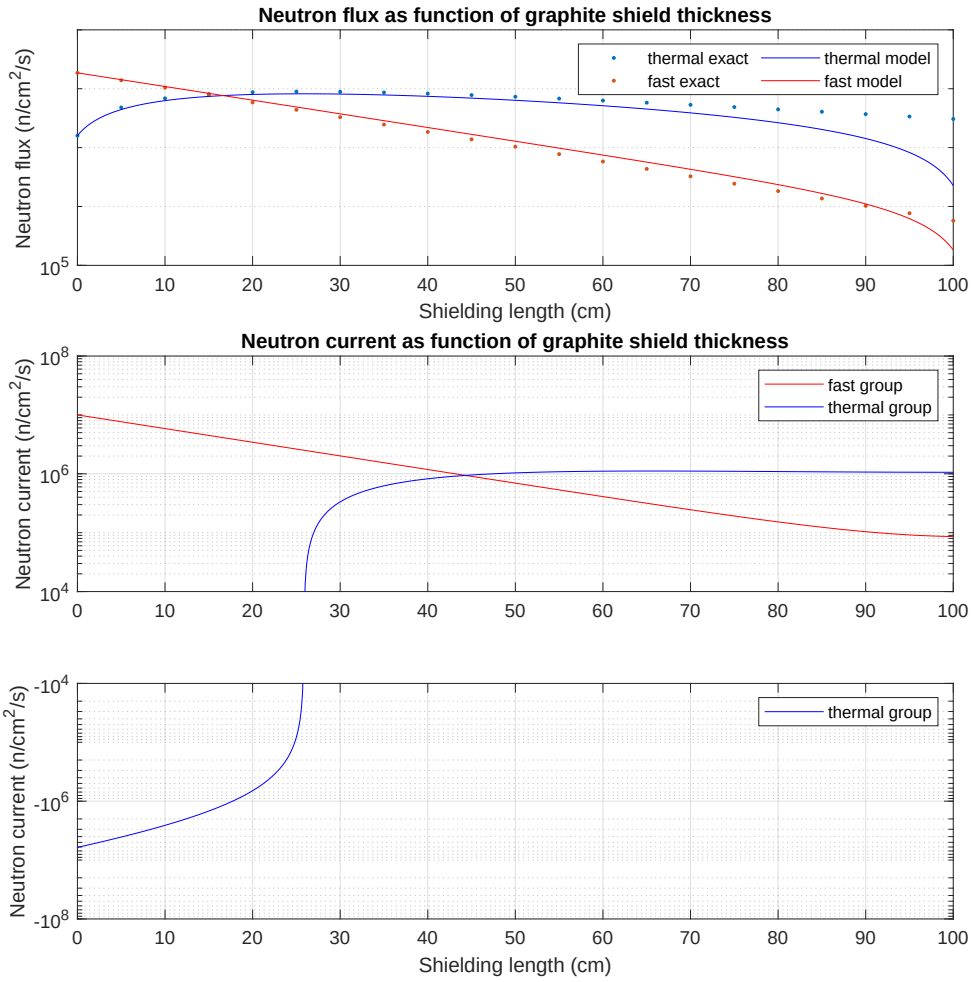

Figure 3.3: Neutron flux (top) and current (middle and bottom) as function of graphite shield thickness of fast and thermal neutron group, comparing transport model results with exact theoretical values.

Firstly, the thermal neutron current is negative for the first part of the shielding. This can be explained because there are no thermal neutrons entering the shield from outside, so all thermal neutrons are 'born' within the shield. After their 'birth' they start to diffuse to the outside thus creating a negative current in the first part of the shield. Based on this insight it may not be a good idea to make the first part of the shield of a material that a good moderator but a bad absorber. Otherwise thermal neutrons start leaking back into the machine.

Secondly, the model is run with graphite. This material is used in fission reactors because it is a very good moderator and a bad absorber. Consequently the thermal neutron current does not decay significantly towards the end of the shielding, thus making it a useless shielding material.

3.3 Materials

In literature, a variety of neutron shielding materials are found. Their performances are linked to the neutron source with which they were tested (computationally or experimentally). To find out

Material	Formula	Density g/cm^3	Required thickness fast neutrons cm	Required thickness thermal neutrons cm
Concrete				
Ordinary concrete		2.25	312	240
Magnetide boron concrete		3.05	219	127
Water	H_2O	1	159	126
Hydrocarbons				
HDPE	$(CH_2)_n$	0.92	133	105
5% borated HDPE	$(CH_2)_n$, B	1.07	114	58
30% borated HDPE	$(CH_2)_n$, B	1.19	101	35
5% borax-paraffin	C_nH_{2n+2}, B	1	123	79
Advanced materials				
Zirconium hydride	ZrH_2	5.6	123	100
Zirconium borohydride	$Zr(BH_4)_4$	1.18	118	39
Titanium hydride	TiH_2	3.77	106	68
Magnesium borohydride	$Mg(BH_4)_2$	1.48	68	23

Table 3.2: Required shielding thicknesses for different materials shielding neutrons of 7 MeV and flux of $1 \cdot 10^8$ n/cm^2/s, as calculated by the neutron transport model.

which shielding material has the highest performance against 7 MeV neutrons, a list of potential shielding materials is composed, and all of them are tested with the neutron transport model. The materials that are categorized in the same way as in section 2.4: concrete, water, hydrocarbons and advanced materials. Table 3.2 shows the best of each category.

The materials are tested with the neutron transport model with a flux of $1 \cdot 10^8$ n/cm^2/s and neutron energy of 7 MeV. The flux as function of shielding thickness is calculated and the thickness at which the flux falls below the legal limit of 1 n/cm^2/s. The fast and thermal neutron flux are calculated separately, and thus each result in their own required thickness. Because both fluxes have to be below the legal limit, the largest thickness of the two determines the minimal required thickness. When the required thickness for thermal neutron is smaller than that of fast neutrons, it means that the neutron absorption of the material is so good that behind that thickness, fast neutrons slow down too slow to raise the thermal flux above the limit. And the fast neutrons that do slow down, are absorbed fast enough.

From all the materials in table 3.2, magnesium borohydride has the best performance. However, for this material the price was found to be 146 euro/gram. The rest of the advanced materials perform approximately similar to the hydrocarbons. With more boron added to the material, the required thickness for thermal neutrons decrease significantly, but in that case the required thickness for fast neutron is decisive. The two concretes do not perform as well as expected, considering that concrete the most commonly used neutron shielding material. The reason for this is that the shielding relies on inelastic scattering and multiple materials working together due to their different resonance peaks. However, inelastic scattering is not included in the transport model, and due to averaging of cross sections over a energy range, this cooperation of resonance peaks is not accurately replicated.

Based on these results, the materials HDPE and b5-HDPE are selected as main shielding materials because of their good shielding performance, light weight, and possibility to process easily. Because of the low density, HDPE is not a good gamma stopper. With the addition of boron, a big part of the gammas that are emitted have a lower energy, because the capture reaction with boron emits a lower energy photon than the capture reaction with hydrogen. However, the

environment still needs to be shielded from this gamma radiation. Designing proper shielding for this radiation is left for future work.

With the implemented neutron transport model, it is not possible to implement different shielding geometries. To design and test a geometric design, a Monte Carlo code is used. The chapter 4 explains the simulation configurations of this code. Subsequently, in chapter 5 the neutron shielding is designed and the performance is simulated with the Monte Carlo code.

Chapter 4

Simulation configuration

With the knowledge of neutron transport and good shielding materials, the next step is to make a shielding design. To test whether a design fulfills the requirements, it is tested with a Monte Carlo neutron transport simulation. Results of test simulations are used for the iterative process of designing the shielding. In this chapter, first the transport code is introduced. Subsequently, the iterative process is explained. And finally, the setup of the codes configurations are explained.

4.1 MCNP

To test the shielding performance of a design, the design is implemented into MCNP and the neutron transport is simulated. MCNP stands for Monte Carlo N-Particle code [a]. The code is developed by Los Alamos National Laboratory in the United States, starting of with neutron diffusion and multiplication calculations in the nineteen-forties [b]. The code is now capable of calculating the transport of many particles with even more types of particle interactions, but in this work it is used mainly for its original purpose: neutron transport and interaction.

4.2 Design process

The first step is to implement the Dynaxion neutron source into MCNP and see whether MCNP simulates what we expect of it. Then, a collimator is drawn around the source to stop the neutrons that are not needed as close to the source as possible, effectively making the neutron beam. Subsequently, a beam stop is placed behind the package to stop the high flux of high energy neutrons that finished their job of going through the parcel. At this point, the design is such that neutrons go through three machine components (collimator, parcel, beam stop) in which they are scattered. As a result, the neurons that bounce around in all directions form some sort of background neutron radiation noise. The outside world needs to be protected from this background flux and this is done by changing two things of the design: 1) current components are optimized to reduce scattering, and 2) an overall shield is designed that encompasses the full system. Finally, all components need to work together in shielding neutrons, because there is no point in optimizing one component, when neutrons scatter of the other in all directions. Within every step, multiple designs are tested. And based on simulation results, what is learned can be applied to upgrade the design, and test again. This iterative process has proven to be essential because insight on where its best to put material, and where not was only learned while doing simulations.

4.3 Source Implementation

The source spectrum was calculated using the DROSG code. Its data was provided in the form of a list of data points outlining a 3D surface that represents the neutron yield as function of direction and energy. It is not possible to simply feed this list into the MCNP input file, so some processing had to be done.

For the Dynaxion source, the probability of a source neutron having a certain energy and direction is dependent on those two variables. In MCNP, this can be implemented by entering a probability distribution for variable 1. Then, every value that variable 1 can take, is given its own probability distribution for variable 2. The provided source data has 180 possible directional values and many more possible energy values. Therefore, the direction is chosen first with a certain probability, and every direction has its own energy distribution.

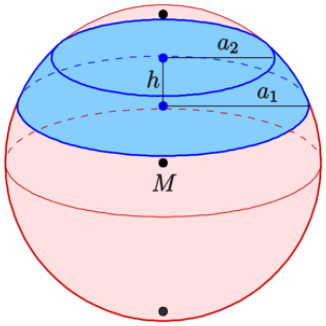

Figure 4.1: Area of a spherical segment

The distribution function are implemented as a histogram with constant values for every bin. To make the directions and energies of simulated source particles continuous, MCNP integrates over the bins of the entered distributions. Here arises a problem. Because of the axisymmetry of the neutron source, the direction distribution curve does not merely describe the probability of a neutron going in one direction, but the probability of it going in a ring of directions around the symmetry axis. And integration between two points thus describes an area on a sphere with the shape of a spherical segment, see figure 4.1.

This surface of a spherical section is called a spherical zone, and its area can be calculated with:

$$A_{zone} = 2\pi Rh \tag{4.1}$$

where R is the radius of the sphere, and h is the width of the spherical segment. The width can be calculated from the desired directional values by:

$$h = R(\cos\theta_1 - \cos\theta_2) \tag{4.2}$$

where θ is the angle of the direction. Since MCNP normalizes the distribution automatically, the absolute values of the set distributions are not important, but only the relative values. Therefore it is possible to divide the spherical zone by the total area of the sphere to get rid of the R in the equation. What is obtained is the fractional solid angle (fsa), given by:

$$fsa = \frac{A_{zone}}{A_{sphere}} = \frac{2\pi R^2(\cos\theta_1 - \cos\theta_2)}{4\pi R^2} = \frac{\cos\theta_1 - \cos\theta_2}{2} \tag{4.3}$$

With this, a distribution histogram is obtained by taking the original data, finding the average value in all bins, and multiplying it by the fractional solid angle of the bin.

4.4 Source Bias

The solid angle integration from the previous section has a counterintuitive consequence, which can be best explained by temporarily using an isotropic source as example. An isotropic source is by definition axisymmetric. Thus, a directional distribution can be described as a function of only the angle between the axis and the direction. This distribution is not uniform, but it is highest at a 90 degree angle, and approaches zero at 0 and 180 degrees. It follows the relationship of equation 4.3 to be precise. The conclusion that can be drawn from this is that even for an isotropic source, many more neutrons are going side ways than there are going forward or backward. Because

MCNP is a Monte Carlo code, the number of neutrons calculated going in a certain direction is proportional to the actual directional distribution. And in an axisymmetric problem this results in acquiring much more information about the sideways direction than the forward direction.

Going back to the Dynaxion source, the exact distribution of the source differs from an isotropic source, but the consequence is the same. On top of this disbalance in information, in many of the coming simulations, the forward direction will actually be of most interest.

MCNP does have a useful tool that can be used to counter this problem. It is called 'source bias'. This tool enables the user to do more calculations in some parts of the source distributions, thereby changing the statistics of the simulation outcome, but without changing the essence of what is calculated. Next to the actual distribution, a bias distribution is set to invoke the tool. In this work, the source bias is only used for the directional distribution, and is employed in two different ways. The first is to exactly counteract the solid angle problem by setting the bias distribution to the inverse of the direction distribution of an isotropic source. And the second is to simulate many more neutrons going in the forward direction, which was used when simulating the beam stop. Because this way, more computation time is spend on calculations of neutrons reaching the beam stop, making the calculations in this region more efficient (more information with fewer source particles).

4.5 Geometry

Making a geometric design for the shielding does not start with a blank page. The system components, as they are envisioned right now, set design constraints. First, there is the particle accelerator. Its exterior is beam shaped, with an approximate length of 2 meters and diameter of 50 centimeter. Between the accelerator and the neutron source target, there is a 30 centimeter long aluminium deuterium beam exit with a diameter of 10 centimeter. The source target and subsequent neutron beam exit are determined to have the same 10 centimeter diameter. And some distance behind the target should be room to place the tested parcel. The length of the neutron beam exit that sets this 'distance', should be made as short as possible, to maximize the number of neutrons reaching the parcel, but will be limited by the shielding capacity of the collimator, as explained in the next chapter. For the parcels, a room of approximately 1 meter in all directions and space to get them there must be reserved. And finally, also measuring systems must be placed somewhere around the parcel. Although the exact dimensions and placements of these systems are not fixed yet, their placements must be taken into account.

Implementing geometries into MCNP is done as follows: First, surfaces are defined. Different kinds of surface are available (e.g. plane, cylinder, sphere, cone). In the input file, the surfaces are selected, positioned and oriented. Second, three-dimensional cells are defined by enclosing a volume through referring to the surfaces. Subsequently the cell gets assigned a material with a density. Then, for every cell, the particle 'importances' are entered. A particle importance of 1 means that the tracks of this type of particle are calculated, and 0 means the particle is killed. The particle importances are a way to restrict the extent of the simulated volume.

Another way to restrict a simulated volume is to implement reflective surfaces. When a particle is going to pass through this surface, it is reflected perfectly. As if it would have went on to an adjacent mirrored cell. In this case of volume restriction the particle is not killed, but kept and its track is simulated further. Therefore, it can be used to introduce symmetry.

It is already explained that the neutron source is axisymmetric. Furthermore, the particle accelerartor, accelerator beam exit, and target are also axisymmetric. And for the other components, the shapes are not yet fixed. It is not probable that the measuring systems and parcel movement system will be axisymmetric, but since they have yet to be designed, it is impossible to include them in the simulation already (only space must be reserved). That leaves the collimator, beam stop, and overall shielding, and at this point of the design process there is no reason they cannot be axisymmetric.

This axisymmetric design is easiest to describe with a cylindrical coordinate system ($\rho\phi z$). In this system the source is placed such that the main neutron beam coincides with the positive

z-direction. Because of the axisymmetry, the geometry is uniform in the second dimension (ϕ). An MCNP simulation will shoot neutrons from the source in every different ϕ direction. However, due to the uniformity of the geometry in the second dimension, the information that is gained from neutrons going in any direction ϕ is also applicable in all other directions.

Due to this property, all points in the simulation with the same ρ and z value (with ϕ values ranging from 0 to 360) can be averaged to one value without losing information. This way, the simulation is effectively made 2D, and more precise simulations can be done more efficiently.

4.6 Materials

The materials that are assigned to the cells must be defined in the third block of the configuration file. The user has to define materials themselves and give every material its own material number that can subsequently be used in the rest of the code. A material is defined by selecting all the isotopes that the material consists of, and for every isotope the abundance in the material. No density has to be given at this point, because the density has to be assigned later for every cell individually. This is to give users the opportunity to use materials at different pressures and temperatures without having to assign a different material for each of the occurring densities.

For some elements, MCNP knows the natural occurring abundance per isotope, and in that case an element instead of multiple isotopes could be selected to define a material. But for most elements, ENDF does not have cross-section tables for the naturaly occuring isotope abundances, and therefore every isotope had to be selected individually. Also, a few materials, like water and HDPE, have deviating cross-sections around thermal temperatures. For these materials a seperate ENDF library could be selected to account for these deviations.

4.7 Tally

While simulating, MCNP gathers a lot of data. Not all this data is saved. In fact, by default MCNP saves as little as possible. Instead, it gives users the possibility to select only data that is of interest. The saved data can be exported to be processed by any adequate software package, or it can be processed by the included MCNP plotter environment. This plotter is very basic in its capabilities, but the advantage is that it ready to be used.

The most rigorous option of saving data is saving all the particle tracks. Due to the size of the output files MCNP discourages this. Besides, the plotter environment does not process the particle track files. However, saving all the particle tracks would have given the opportunity to do extensive analysis with Matlab, offering more freedom. This option was not chosen because building processing software would have taken a lot of time, while the plotter environment is adequate for the intended use.

The conventional option of saving data is using tallies. Tallies are virtual counters that only save data from selected regions, energies, particles, etc. They come in different shapes (surfaces, volumes, and meshes) that can be placed in the geometry. Particles going through a surface or volume tally, are counted, and the desired information about them is saved. To give an example: a volume tally can measure the neutron flux in particles/cm2 in a certain volume.

As is explained in the previous section, the simulations are done in 3D but the results are interpreted as a 2D problem. This can be achieved by averaging the results from the third dimension into one value. With the tallies, a shortcut can be taken: the data of the third dimensions is not saved in the first place. For this, mesh tallies are used. Mesh tallies create a 3 dimensional mesh of volumes that are all tallied individually. In this work, a cylindrical mesh tally is placed with its axis on the axisymmetry axis of the system. Then, the polar and longitudinal directions are divided in sections of 1 centimeter, while in the angular direction, there is only 1 bin. The resulting tally can thus be depicted in a 2 dimensional plot.

4.8 Simulation

Finally, in the MCNP configuration file all simulation settings and countless complex tools can be evoked. This section explains all the settings that were used in this work.

First and foremost, the user can choose which particles are to be simulated. There are a few dozen options, but in this work mainly neutrons, and sometimes gamma's are run. Simulating neutrons, means that only neutron tracks are calculated, together with all the interactions they can have with all particles that are part of the defined materials. In MCNP, neutrons only interact with nuclei, not with eachother and not with themselves. Meaning there are no neutron-neutron interactions, and neutrons do not decay. For an inelastic scattering event, for instance, it is noted that a gamma is produced, but its track is not followed. For that, the gamma setting should be turned on.

Furthermore, the user can choose the number of source particles that are simulated. One source particle may cause a whole range of other particles to be born (other neutrons, photons, or fission products) and depending on the settings, the particle tracks of these particles are either followed or not. Simulating more source particles takes more time, but it can decrease the variance of the measured values.

The upper and lower energies of every particle can be entered. When a neutron somehow gets a higher or lower energy than the chosen range, MCNP uses tables to simulate their behaviour, instead of calculating all the relevant physics. For neutrons there is another way to reduce the variance of the measured values, and that is setting implicit or analog capture. With analog capture, a neutron is killed when the lottery decides it is captured. But with implicit capture, a source neutron gets a weight of 1, and every time there was a chance of it being captured, their weight is reduced. With this trick, simulated neutrons reach regions for which they had a very low chance to reach it, but the reduced weight ensures that the right odds of the particle reaching a tally are known.

Chapter 5

Neutron shielding design

Three shielding components (collimator, beam stop, and overall shielding) have to work together to meet the design requirements. These requirements are explained in section 5.1. It is not fixed which component is responsible to shield what part of the radiation, and every shielding component influences the number of neutrons reaching the other components. Additionally, a parcel in the beam also influences the flow of neutrons through the system. Therefore, in the subsequent sections, the components are designed and simulated one by one, in the order of which is closest to the neutron source.

5.1 Design requirements

Based on the requirements of the Dynaxion system that are explained in the introduction, the following requirements for the neutron shielding design are set:

1. The most important requirement of the neutron shielding is that the neutron radiation outside of the machine does not exceed the legal limit of 1 n/cm^2/s. The tallies, that are used for flux measurements in the simulations, normalize their measurement by the number of source particles that are used for the simulation. The resulting values are therefore given in cm^{-2}. Since the Dynaxion source produces 10^{10} n/s, the maximum normalized neutron flux outside of the machine is 10^{-10} cm^{-2}.

2. The number of neutrons bouncing around (ambient neutrons) in the system must be limited for multiple reasons:

   - ambient neutrons can cause inelastic scattering reactions outside of the parcels region of interest, complicating the scanning process.
   - lifetimes of system components are negatively influenced by neutron irradiation
   - a solution for loading and offloading parcels must be designed, which is expected to place stringent requirements on minimizing the ambient flux

   However, since the system is in the proof of concept phase, a maximum value for the ambient flux is not set. Therefore, the design is aimed at minimizing the ambient flux to find out what ambient flux is to be expected, and what it takes to reduce it.

3. The shielding solution has to leave enough room for the system itself, including: a conveyor belt that transports packages of up to 60 cm in diameter, detectors with collimators. Additionally, all machine parts have to be reachable for maintenance. Therefore for the parcel, a space of 1 m in diameter has to be reserved. However, for the other components, no dimensions are fixed.

4. To meet the requirements of the system being light, compact, and transportable, the volume and mass of the shielding have to be minimized. The maximum total volume of the machine is aimed at the size of a standard shipping container (6x2.4x2.4 m). The size of other system components is not known yet, meaning there is no clear size limit for the collimator. The outer edges of the overall shielding however, are constrained to the mentioned shipping container dimensions.

5. To meet the requirement of financial viability, the total system cost has a maximum on the order of a million euros. For the shielding material, this means that the estimated cost have a maximum in the order of a hundred thousand euros.

5.2 Collimator

The scanner has to shoot high energy neutrons to a region of the parcel, but outside of that region it needs none. The source, however, emits neutrons in every direction. Guiding neutrons that are emitted in the wrong direction towards the parcel is not possible, so these are redundant and have to be stopped. Stopping redundant neutrons can in principle be done by the overall shielding. However, the number of neutrons bouncing around (ambient neutrons) in the system must be limited. Therefore, it is best to shield the redundant neutrons close to, and all around the source.

At the same time, neutrons that are emitted in the right direction have to reach the parcel uninterrupted. They can do that through the neutron beam exit, a hole in the collimator. The shape of the neutron beam exit influences which neutrons are stopped and which can go through. Thus, the collimator shapes the neutron beam.

The optimal size of this region has not been determined yet, but it is expected to be in the order of 10 cm. In this work, the desired beam diameter is set to 10 cm at 1 meter from the source. To radiate the parcels region of interest precisely, within that beam, the neutron flux has to be as high as possible, and outside of it as low as possible. To achieve this, the edges of the beam profile (neutron flux as function of radial distance from the symmetry axis) have to be steep.

5.2.1 Simple collimator

The first design is made as simple as possible, see figure 5.1. Since the simulation is set up as an axisymmetric problem, the simple collimator design is axisymmetric as well. The collimator is a hollow cylinder with its axis along the axisymmetry axis. The hole of the cylinder houses the 30 cm long aluminium accelerator beam, the neutron source, and the neutron beam exit, all with an outer radius of 5 cm. Furthermore, for now, the outer radius of the collimator is set to 50 centimeter and the total length to 130 cm, because test simulation have shown that this is enough to lower the neutron flux by $5 - 8$ orders of magnitude. A much smaller collimator would not shield enough, but a much larger collimator is unnecessary because the neutrons that are not stopped can still be stopped by the overall shielding. The shielding material of the collimator is HDPE.

In order to evaluate the collimator performance, the following metrics are used: the shape of the beam profile, the energy spectrum of neutrons leaving the collimator, and the neutron flux throughout the simulated space. The latter is measured with the cylindrical mesh tally (section 4.7). From this, also the beam profile is obtained. It is measured at 1.5 m from the source, where it should have a diameter of 15 cm. The energy spectrum of neutrons leaving the collimator is measured on three different positions: at 1.5 meter from the source both inside ($r < 7.5$ cm) and outside ($7.5 < r < 50$ cm) of the beam, and along the side of the collimator ($r = 50$ cm, and $-30 < x < 100$ cm). The simulation is run with $1 \cdot 10^7$ source neutrons.

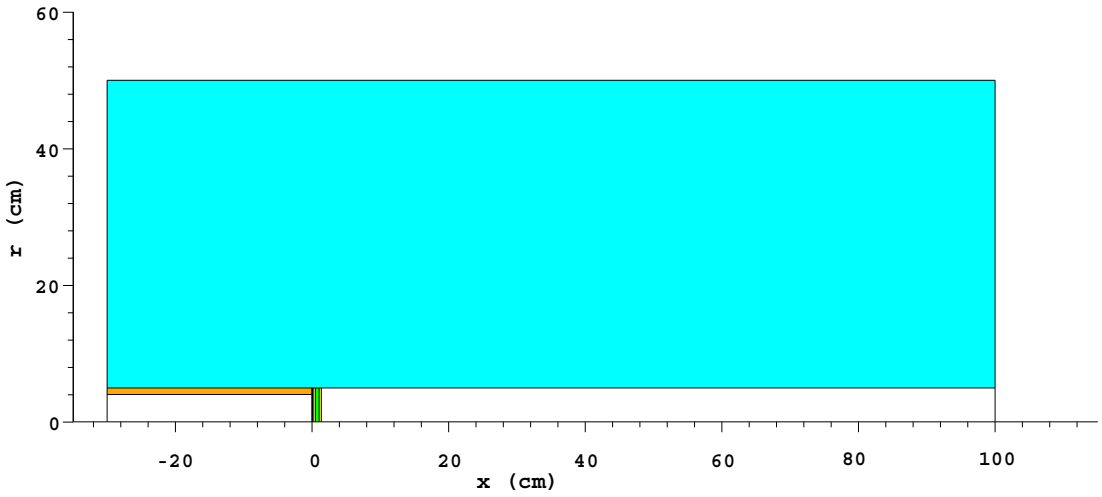

Figure 5.1: Schematic overview of simple collimator design in a cylindrical coordinate system, where x is the symmetry axis, and r the radial direction. White represents the vacuum, orange the aluminum accelerator beam, and light blue the HDPE collimator. The neutron source consists of various materials and is positioned at $0 < x < 1.6$ cm.

Results

The neutron flux throughout the simulated space is plotted in figure 5.2 for two simulations. Firstly, the neutron source without any material around it, and secondly, the neutron source with the simple collimator. The colors represent normalized neutron flux in cm^{-2}, so when the simulation is done with a different number of source neutrons, the results have the same unit. The Dynaxion source emits 10^{10} n/s, so the legal dose limit of 1 $\text{n/cm}^2\text{/s}$ corresponds with a normalized flux of $1 \cdot 10^{-10}$ cm^{-2}. The figure reveals the following things:

Figure 5.2: `<redacted>`

- The neutron flux decreases very fast as function of the distance from the source. This can be seen in both the simulation without collimator and in the beam of the simulation with collimator. The reason for the steep decline of intensity is that although the collimator effectively narrows the beam, it is still a diverging beam. The intensity of the beam scales with the inverse of the area of a sphere, known as the inverse-square law, which is given by:

$$I \propto \frac{1}{r^2} \tag{5.1}$$

in which I is the intensity of the neutron radiation and r the distance from the source. Figure 5.3 shows the neutron flux as function of distance from source for an isotropic source (theoretical), and the uncollimated and collimated Dynaxion source (simulated). The flux of the Dynaxion source is one order of magnitude higher than the isotropic source because of the skewed angular distribution, but the trend follows the inverse-square law of equation 5.1. Therefore, without shielding material between the source and the parcel, the neutron flux at the parcel depends solely on the source flux and the distance to the source. To increase the flux at the parcel, it has to be placed closer to the source, requiring the collimator to be shorter.

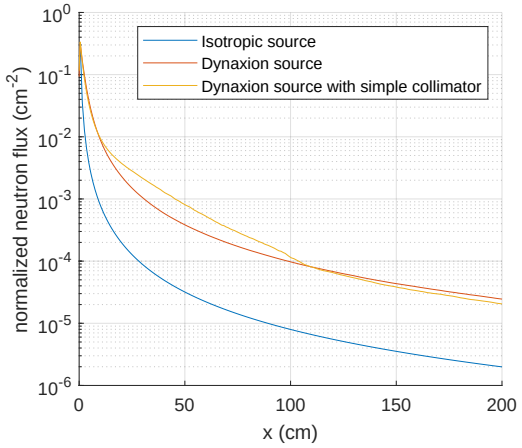

Figure 5.3: Normalized neutron flux in cm^{-2} as function of distance x (cm) from the source of: a theoretical isotropic source, compared to the simulated collimated and uncollimated Dynaxion source.

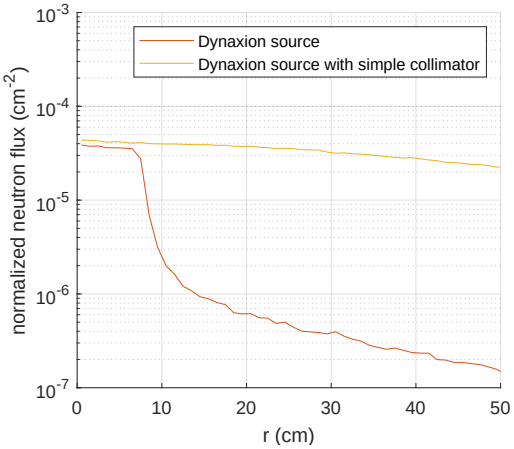

Figure 5.4: Beam profile, measured in normalized neutron flux (cm^{-2}) as function of distance r (cm) from the symmetry axis at $x = 1.5$ m.

- The collimator has successfully created a beam profile. Figure 5.4 shows the beam profile at 1.5 m from the source for both the collimated and uncollimated Dynaxion source. At 1.5 m, the beam has a width of approximately 7.5 cm, and the profile has a steep edge. Furthermore, the flux of the collimated beam is slightly lower than the uncollimated beam, but this is explained by the latter also having no source materials present in the simulation. Outside of the beam, the neutron flux is around 2 orders of magnitude lower for the collimated beam than the uncollimated beam. The next design is aimed decreasing the neutron flux outside of the beam and increasing the steepness of the beam profile.

- All sides of the collimator emit neutron radiation because there is not enough shielding material to stop them all. To analyse what are the energies of the neutrons flowing out of the collimator, neutron energy spectra are measured in three positions. The results are depicted in figure 5.5. The spectrum at the side of the collimator shows that high energy neutrons are slowed down by the shielding material, resulting in a distribution of neutrons over all energy bins. The lower neutron energy, the lower the neutron flux because at lower energies, the elastic scattering cross section increases. Therefore, neutrons lose their energy quicker than neutrons with a higher energy. However, once the thermal energy is reached, the neutrons on average stop losing energy, explaining the increased flux around the thermal energies. The flux peak around thermal energies is also present in the beam spectrum and out-of-beam spectrum.

Borated HDPE

Many thermal neutrons are not captured before they escape the collimator shielding material. In the materials chapter it was shown that b5-HDPE is better at capturing neutrons and thus lowering the neutron flux of low energy neutrons. By changing the material in the simulation from HDPE to b5-HDPE this effect can be shown in practice. Figure 5.5 shows the neutron spectra of the collimator with b5-HDPE as shielding material compared to HDPE. The results show that the flux of the thermal neutron peak is decreased by around 2 orders of magnitude. These low energy neutrons do not necessarily have to be stopped by the collimator; maybe the beam stop or overall shielding are better suited to do this job. But for the remainder of this report, the collimator is made of b5-HDPE because then origins of thermal neutrons are more easily deduced from simulation results.

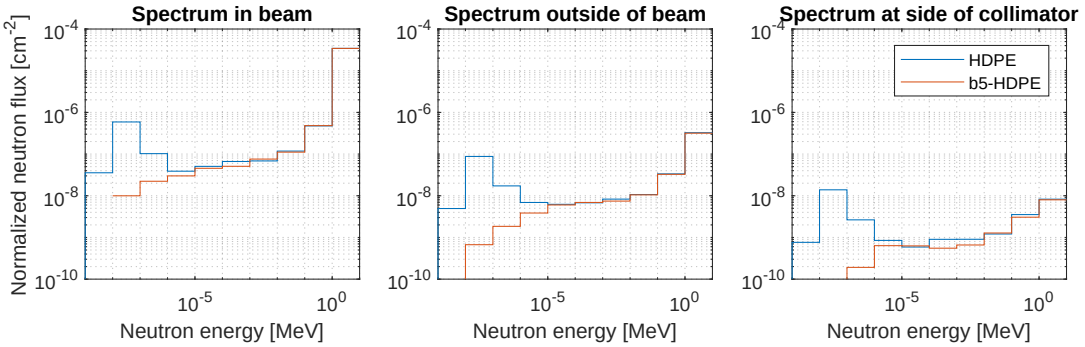

Figure 5.5: Neutron energy spectra of three different surfaces from left to right: in the beam ($r < 7.5cm$) at 1.5 meter from the source, outside of the beam ($7.5 < r < 50cm$) at 1.5 meter from the source, and along the side of the collimator.

5.2.2 Beam shaping

In the previous section it was concluded that the beam profile shows a steep edge and low neutron flux outside of the beam. However, the middle plot of figure 5.5 shows that just outside of the beam, there are many more high energy neutrons present than lower energy neutrons. With the current collimator design, neutrons leaving source heading in a direction just outside of the intended beam direction, encounter little shielding material: namely the outer corner of the neutron beam exit. As a result, these neutrons do not have enough elastic scattering collisions to be stopped by the collimator. Instead, they leave the collimator with a high energy and in every direction because of the deflections of the collisions they did have. However, if the collimator is designed such that these neutrons already collide at the center of the collimator, there is enough shielding material around it to stop and absorb them. To stop all the redundant neutrons in the center without effecting the neutron beam, `<redacted>`

`<redacted>` (5.2)

`<redacted>`

Figure 5.6: <redacted>

The updated design is simulated with $1 \cdot 10^7$ source neutrons. The resulting neutron flux throughout the simulated space is shown in figure 5.6. Below, three improvements are explained:

- The highest neutron fluxes (in red) are limited to the region close to the neutron source. In the simple collimator this region of high flux expanded further towards the end of the neutron beam exit (figure 5.2). The reason for this is that the inner edges <redacted> neutron beam exit are irradiated less directly from the source. <redacted>
- Figure 5.7 shows the beam profile of both the collimator with cylindrical and <redacted> (and two other designs of the next section). The neutron flux outside of the beam profile is a factor 20 lower for the new design. <redacted>
- What is not well visible in figure 5.7 is a 5% decrease in neutron flux inside of the beam. To better understand the reduced flux in the beam, the left plot of figure 5.8 compares the energy spectra of the neutron beam flux of the simple and <redacted> design. Note that the flux of high energy neutrons (> 1 MeV) is not decreased, while the flux of neutrons with energies below 1 MeV is decreased significantly. For the scanning system, only neutrons

with energies above 1 MeV are needed because below these energies the cross sections for inelastic scattering are too low. Therefore, the 5% decrease of neutron beam flux does not negatively impact the scanning system.

Figure 5.7: Normalized neutron flux as function of distance r from symmetry axis for two collimator designs: the simple collimator with cylindrical neutron beam exit, and the updated design with `<redacted>` neutron beam exit.

Figure 5.8: Neutron beam energy spectrum at $x = 1.5$ m for $r < 7.5$ cm of two collimator designs: the simple collimator with cylindrical neutron beam exit, and the updated design with `<redacted>` neutron beam exit.

5.2.3 Volume optimization

The radius of the cylindrical collimator was arbitrarily set to 50 cm. Figure 5.6 shows that there where is more shielding material between the source and the edge of the collimator, the neutron flux at the edge is lower and fewer neutrons flow out of the collimator. This part of the collimator thus contributes less to the ambient flux. Since the neutron flux decreases exponentially as function of the shielding thickness, extra shielding material is best placed on surfaces where the escaping neutron flux is highest. Because there, the most neutrons are stopped with the least amount of shielding volume. Therefore, the optimal outer shape of the collimator follows a neutron flux contour line.

Placing extra shielding material will reduce the ambient flux. However, this comes at the cost of the larger volume of shielding material. Therefore, there is a trade-off between ambient flux and shielding volume. For both the shielding volume and ambient flux, the design requirements do not state fixed maximum values. In this work, the ambient flux is therefore set to $5 \cdot 10^{-8}$ cm^{-2}, based on the ambient flux that is caused by the beam stop of section 5.4. However, in the future, this trade-off can be optimized, when more information is available on the system design and the maximum tolerable ambient neutron flux.

In order to keep the collimator design simple while approaching the optimal shape, the collimator is subdivided into 13 cylinders with $dx = 10$ cm. Every cylinder is given its own radius dr based on the required shielding thickness. These values are distilled from the the flux field of figure 5.6, of which the contour line of $5 \cdot 10^{-8}$ cm^{-2} is plotted in figure 5.9. The updated collimator design is depicted in the same figure.

Figure 5.9: Schematic overview of volume optimized collimator design, where x is the symmetry axis, and r the radial direction. The wriggly line is the contour line of $5 \cdot 10^{-8}$ cm^{-2} from the simulation of figure 5.6. White represents the vacuum, orange the aluminum accelerator beam, and light blue the b5-HDPE collimator. The neutron source consists of various materials and is positioned at $0 < x < 1.6$ cm. *Note: figure has been* `<redacted>`

5.3 Parcel

After the beam leaves the collimator, it goes through a parcel. Because the neutrons scatter on its material, the parcel influences the neutrons flux throughout the machine. This section explores the extent of this influence. Simulations are done with the neutron source, the collimator and parcels with different materials and sizes. The parcels are positioned with their center at 50 cm from the neutron beam exit. To keep the exercise as simple as possible, the parcels are cylindrical

and oriented in the beam such that the axisymmetry is not lost. Furthermore, they are made of only 1 material. The chosen materials and dimensions are given in table 5.1, and explained in the next paragraphs.

Four parcels were chosen to represent a normal parcel. No extensive research is done on what exactly the average parcel looks like, but it was found that most parcels weigh less than 2 kilograms [a] and that the most commonly transported packages contain clothing, books, cd's, and food [b]. Based on this, the first three parcels are made of paper (by weight: 32% C, 4% H, 51% O, 6% Ca, 4% Al, 2% Si, and 1% Ti), plastic (C_2H_4), and water (H_2O). They have a fixed size and weight and thus the density of the material was adjusted accordingly. The fourth parcel was made to resemble a suitcase with clothes. This cylindrical parcel is made of cotton cellulose ($C_6H_{12}O_6$), with the dimensions and weight of a suitcase, and the density adjusted accordingly.

Furthermore, five parcels were chosen to find a worst-case scenario, in which a maximum number of neutrons scatter and do not end up in the beam stop. Instead, they must be stopped by the overall shielding, which is costly because of the larger volume. Five materials with high neutron cross sections were chosen: copper, lead, iron, plastic, and water. These materials are solid, have their actual material density, and a weight around the $50 - 70$ kg.

In order to quantitatively compare the influence of the parcel on the neutron flux, two surfaces are selected for the comparison. The influence on the neutron beam is measured 1 m from the neutron beam exit. There, a circular surface tally is placed normal to the symmetry axis with a diameter of 20 cm, matching the size of the beam in that position, see figure 5.10. The parcels influence on the ambient neutron flux is measured 50 cm from the symmetry axis. There, a cylindrical surface tally is placed ranging from 0 to 100 cm from the neutron beam exit, see figure 5.10.

Figure 5.10: Schematic side view of the simulation setup. On the left side the collimator with `<redacted>` shaped neutron beam exit in light blue, right of it the parcel in pink, and all around it the vacuum in white. Black lines represent surface guides that are used to define cells and tallies. The surface tallies that measure beam flux and ambient flux are highlighted with yellow. *Note: figure has been `<redacted>`*

5.3.1 Results

The results of the ten different simulations are shown in figure 5.11. For the normal parcels,the in-beam neutron flux is decreased by a factor 2 to 4 . This means that approximately $50 - 75$ % of the neutrons in the beam collided at least once with the parcels material. One collision is not enough to slow them down to thermal speeds, but it does result in a change of direction. Therefore, these neutrons leave the parcel in many different directions while still having a high energy. Consequently, they need to be stopped by the overall shielding. This is confirmed by the

measurements of the ambient neutron flux. Compared to the baseline measurement without a parcel, the ambient neutron flux has increased by more than an order of magnitude. Comparison between the normal parcels also shows that the more the in-beam neutron flux is decreased, the more the ambient neutron flux is increased.

material	diameter cm	height cm	weight kg	density g/cm^3
<redacted>				

Table 5.1: <redacted>

Figure 5.11: <redacted>

For the worst-case parcels, the in-beam neutron flux is decreased by $1.5 - 2.5$ orders of magnitude. But for the metals, the ambient neutron flux is only slightly higher than with the normal parcels. The difference is so small because with the normal parcels $50 - 75$ % of the neutrons are removed from the beam and for the worst-case metal parcels $95 - > 99$ %, not more than a factor two difference. However, in the high density metals, neutrons collide more often, and per collision the average change in direction is higher than in the normal, low density parcels. Therefore, in the normal parcels the neutrons only get a minor change in direction and leave through the gap between the two tally surfaces, which explains why the difference in ambient flux is more than a factor two.

For copper and iron, the in-beam and ambient neutron flux are approximately the same, meaning that the neutrons scatter enough to divide them equally over all directions. Therefore it is not possible to find a parcel that increases the ambient neutron flux much more. The reason that this ambient flux does not get higher is found in the inverse squared law. Because so many neutrons are scattered in the parcels, the parcel starts to resemble an isotropic neutron source. From the parcel the neutrons diverge and are spread out over a larger surface, limiting the maximum neutron flux at a certain distance.

For plastic* and water*, the measured ambient neutron flux is even lower. This can be explained by the fact that they are good neutron absorbers. Thus, part of the neutrons that are removed from the beam do not leave the parcel on a different direction but are captured. In the normal parcels this effect is smaller because due to their lower density and smaller size, neutrons are not slowed down enough for the capture cross sections to be significant.

From this analysis the following is concluded: parcels have the capacity to scatter more than 99 % of the beam neutrons. However, for the ambient flux the difference between a normal parcel and a worst-case parcel is a factor $2 - 4$. In the next section it is investigated how much this factor influences the required overall shielding thickness.

5.4 Beam stop

After the neutrons have gone through the parcel, they need to be absorbed. Even though a large percentage of neutrons are deflected by the parcel, the fraction of neutrons going straight through are most difficult to stop. Firstly, because these neutrons still have their original high energy. And secondly, because the neutron beam divergence is smaller than close to the source. In other words, the inverse-square law is less steep this far from the source. Therefore, the neutron flux decrease must come from the shielding material stopping neutrons almost entirely. This section explores the materials and dimensions needed to reduce the neutron flux behind the beam stop to below the legal limit. For this, multiple designs are simulated together with the neutron source and collimator.

The shape of the beam stop is chosen to be cylindrical and it is placed with its axis along the axis of the collimator to satisfy the axisymmetry of this problem. The beam stop is placed 1 m from the collimator to leave enough space for a conveyor belt system that can process parcels with dimensions of up to 60 cm. Initially, the radius of the beam stop is set to 50 cm and the thickness

Design combinations				Simulation results	
Material A	Material B	Length A cm	Length B cm	Required length cm	Normalized ambient flux $\times 10^{-8}$ cm^{-2}
<redacted>				<redacted>	

Table 5.2: <redacted>

to 1 m, see figure 5.12. In this example the beam stop is made of two materials, this is clarified in the next paragraph.

In order to compare different designs quantitatively, the neutron flux inside of the shielding material and the ambient neutron flux are measured. Inside of the beam stop, a mesh of volume tallies is made to measure the neutron flux as function of the beam stop length. This grid has a radius of 20 cm, matching the radius of the beam, and lengths of 5 cm each. The ambient flux is measured at the same position as in the previous section: 50 cm from the axisymmetry axis, between $x = 100$ and x=200 cm.

Figure 5.12: <redacted>

<redacted>

The goal of the beam stop is to reduce the neutron flux behind it to below $1 \cdot 10^{-10}$ cm^{-2}. For a Monte Carlo simulation this means that many particles have to be simulated to accurately measure such low values. Therefore, every beam stop combination is simulated with $1 \cdot 10^8$ source neutrons with source bias (section 4.4) in order to decrease the variance of the measurements.

5.4.1 Results

Table 5.2 shows the results of the simulations. The required beam stop length is based on neutron flux in the mesh tally: the x-value of the left side of the first volume with a normalized neutron flux below $1 \cdot 10^{-10}$ cm^{-2}. <redacted>

Figure 5.13: Normalized neutron flux in cm^{-2} as function of x inside of the beam stop for the first five entries of table 5.2. *Note: the figure was* `<redacted>`

Figure 5.14: Normalized neutron flux in cm^{-2} as function of x inside of the beam stop for the first two entries of table 5.2 and the three metals with $lengthA = 20$ cm. *Note: the figure was* `<redacted>`

`<redacted>`

Figure 5.15: `<redacted>`

5.4.2 Volume optimization

An arbitrary shielding volume was chosen for the initial simple beam stop design. The flux of neutrons flowing out of the machine is limited in the requirements to $1 \cdot 10^{-10}$ cm^{-2}. Using shielding material to reach a lower neutron flux outside of the machine is unnecessary. Therefore, the beam stop shape is optimized to shield enough neutrons with the least amount of shielding material.

The shape of the side of the beam stop that faces the neutron beam is restricted by the space that is needed for the parcel and conveyor system. Therefore, the shape of the other side of the beam stop is used for the optimization. To keep the design simple, the beam stop is subdivided into 10 concentric, hollow cylinders with $dr = 5$ cm. Every cylinder is given their own length dx based on the required shielding thickness. These values are distilled from the flux field of the simulation of section 5.4.1, of which the contour line of $1 \cdot 10^{-10}$ cm^{-2} is plotted in figure 5.16. For this example, only one shielding material (b5-HDPE) is used. The cylindrical outer edge of the beam stop is kept flat because in the next section, the overall shielding is designed around it.

Figure 5.16: <redacted>

5.5 Overall shielding

The last step in completing the shielding is designing the overall shield. This shield has to stop all neutrons that are scattered of the collimator, parcel and beam stop. The neutron flux of the incoming radiation is between $1 \cdot 10^{-8}$ and $1 \cdot 10^{-7}$ cm^{-2}, but the area over which it is spread out is large, stretching from the collimator to the beam stop in order to encompass the entire machine.

Because the highest energy (> 1 Mev) neutron flux is less dominant compared to the energy spectrum of neutrons that hit the beam stop, the shielding material of choice for the overall shield is b5-HDPE. To satisfy the axisymmetry, the main shape of the overall shield is a hollow cylinder with a thickness of 50 cm, see figure 5.17. This thickness is chosen such that it as certain that outside of it the flux is lower than $1 \cdot 10^{-10}$ cm^{-2}. After testing the overall shielding with a

simulation, the thickness is reduced according to the results.
<redacted>

Figure 5.17: Schematic overview of overall shielding of b5-HDPE (light blue) around the accelerator (steel, pink), accelerator beam exit (aluminium, orange), neutron source (around $x = 0$ and $r = 0$), collimator (b5-HDPE, light blue), beam stop (b5-HDPE, light blue), and vacuum (white).x is the symmetry axis, and r the radial direction. *Note: the figure was <redacted>*

Results

The overall shielding design is tested with $1 \cdot 10^9$ source particles in order to be able to measure the lowest neutron flux throughout the machine. The source bias is not used because for this simulation, all directions are of interest and not only the forward direction. Instead, the cell importance of the beam stop and overall shielding are set to 5, compared to 1 for all other cells. When a neutron leaves a cell with importance 1 and enters a cell with importance 5, the neutrons splits in 5 and the track of each neutron is calculated. To compensate for the increase number of neutrons, the weight of each neutron is adjusted and the tallies only count them as $1/5^{th}$ of a neutron. This way, sufficient information is calculated in regions that only few neutrons reach.

With a mesh tally, the neutron flux throughout the machine is measured. The results are shown in figure 5.18. The colors indicate the neutron flux, but for clarification the contour line of $1 \cdot 10^{-10}$ cm^{-2} is included. Outside of this line, the neutron flux is low enough to not surpass the legal limit, and the shielding material outside of this line is unnecessary. <redacted>. Figure 5.19 shows what the final design looks like.

Figure 5.18: Normalized neutron flux (cm^{-2}) superimposed on schematic overview of figure 5.17. The wriggly line is the contour line of the outside legal limit of $1 \cdot 10^{-10}$ cm^{-2}. *Note: the figure was <redacted>*

Figure 5.19: Schematic drawing of cross section of the final neutron shielding design. Light blue represents b5-HDPE and pink the stainless steel deuteron accelerator. *Note: the figure was* `<redacted>`

Chapter 6

Conclusion

Summary and *discussion*

In this work, the steps towards neutron shielding of the Dynaxion scanning system are explained. Firstly, a neutron transport model was made to test shielding materials found in literature with relevant neutron energies of 7 MeV. It was concluded that the plastics are most fit for this application, because concrete is too heavy, water performs worse, and advanced shielding materials are too expensive. High density polyethylene (HDPE) and HDPE with 5% boron were chosen as main shielding material, `<redacted>`. It was also concluded that the neutron transport model did not describe the slowing down process over the energy range of more than six orders of magnitude accurately. Furthermore, the transport model did not include inelastic scattering, and there was no option to make a complex geometry of shielding.

Not including inelastic scattering has limited the application of the transport model. Only after the model was implemented, it was concluded that inelastic scattering is important for the neutron shielding performance of concretes. Furthermore, gamma shielding was not included in the model and the design of gamma shielding was left for future work. Both limitations to the model have negatively influenced the ability to analyse the performance of concretes properly. However, in literature, concretes were not found to be significantly better neutron shielders than the plastics. However, because the plastics' densities are significantly lower (3 to 4 times less) than that of the concretes, in the context of designing light weight shielding the choice for the plastics is adequate. If the

The rest of the design process was done with the help of MCNP. Because of the experience gained with neutron transport models, this Monte Carlo code was not merely a black-box that printed results, but could be used to understand the effects of changing the design.

By simulating the performance of potential shielding designs, the full design was completed step by step.

1. A simple collimator design was improved by making a `<redacted>`. The collimator, helped by the inverse-square law, reduces the neutron flux of neutrons not going in the beam direction from $1 \cdot 10^{-1}$ to $5 \cdot 10^{-8}$ cm^{-2}. Shielding it to even lower neutron flux is not necessary because neutrons that bounce of the parcel and the beam stop raise the ambient neutron flux to approximately that level.

   `<redacted>`

2. The influence of a parcel on the neutron beam and ambient flux was tested. It was concluded that a worst-case parcel does not increase the ambient flux much further than a normal parcel, collimator, and beam stop do.

3. A beam stop was designed to stop the high energy, high flux beam, without bouncing back too many neutrons. `<redacted>`. Therefore, b5-HDPE was chosen for the full beam stop.

With this material, the outer shape of the beam stop was optimized to shield to no more than the legal limit requires. In conclusion, the beam stop decreases the neutron flux from $1 \cdot 10^{-5}$ to $1 \cdot 10^{-10}$ cm^{-2} in 98 cm.

<redacted>

4. Finally, the environment is fully shielded from the neutrons by the overall shielding. The bulk of the neutrons are absorbed by the collimator and beam stop, but a fraction are only deflected and slowed down. This results in an ambient neutron flux around $1 \cdot 10^{-7}$ cm^{-2}, spread out over a large surface. The overall shield spans from the accelerator to the beam stop and is made of b5-HDPE. <redacted>

   The backwards direction of the neutron source is occupied by the deuteron accelerator. No extensive research was done on how to shield the accelerator. In the simulation of the overall shielding design the accelerator was shielded with b5-HDPE. However, it is possible that this would lead to an increase of the accelerator temperature, which limits the accelerator performance.

Conclusion

With the low neutron flux outside of the machine, the first requirement is satisfied. Furthermore, the outside dimensions of the overall shielding fit within a sea container, and the shielding does not rely on it being fixed to the ground. Therefore the size and transportability requirements are met as well. The plastics that are chosen have the lowest density of all shielding materials. Besides, they are commonly used as shielding material, and thus readily available.

In conclusion: the neutron shielding that is designed is compact and lightweight and protects the environment from neutron radiation.

Bibliography

[1] K.D. (Ed.). Kok. *Nuclear Engineering Handbook (2nd ed.)*. CRC Press, 2016. 3

[2] Neutron elastic scattering — definition — nuclear-power.net. https://www.nuclear-power.net/nuclear-power/reactor-physics/nuclear-engineering-fundamentals/neutron-nuclear-reactions/neutron-elastic-scattering/. (Accessed on 04/07/2021). 3

[3] Table of nuclides. http://atom.kaeri.re.kr/nuchart/. (Accessed on 04/05/2021). 3, 4

[4] Fermi age theory. https://mragheb.com/NPRE%20402%20ME%20405%20Nuclear%20Power%20Engineering/Fermi%20Age%20Theory.pdf. (Accessed on 04/07/2021). 4, 5

[5] Multigroup diffusion equations — definition — nuclear-power.net. https://www.nuclear-power.net/nuclear-power/reactor-physics/neutron-diffusion-theory/multigroup-diffusion-equations/. (Accessed on 04/07/2021). 5, 10

[6] D. G. Cacuci. *Handbook of nuclear engineering*, page 925. Springer, 2010. 5

[7] Shielding of neutron radiation — types & uses — nuclear-power.net. https://www.nuclear-power.net/nuclear-power/reactor-physics/atomic-nuclear-physics/fundamental-particles/neutron/shielding-neutron-radiation/. (Accessed on 03/27/2021). 6

[8] Fatma Aysun Uğur. New applications and developments in the neutron shielding. *EPJ Web of Conferences*, 154:01022, 2017. 6

[9] Jacob G. and Fantidis. The comparison between simple and advanced shielding materials for the shield of portable neutron sources. *International Journal of Radiation Research*, 13(4), 2015. 6

[10] Scattering in the laboratory frame. https://farside.ph.utexas.edu/teaching/336k/Newton/node52.html. (Accessed on 04/07/2021). 7

[11] Endf/b-vii thermal data. https://t2.lanl.gov/nis/data/endf/endfvii-thermal.html. (Accessed on 04/07/2021). 11

[12] M.M. Ashraf and A.R. Khan. Shielding calculations for the design of neutron radiography facility around parr. https://inis.iaea.org/collection/NCLCollectionStore/_Public/21/069/21069878.pdf?r=1, 1989. 12